

論文 / 著書情報
Article / Book Information

Title	High-Temperature Equation of State of FeH: Implications for Hydrogen in Earth ' s Inner Core
Author(s)	Shoh Tagawa, Hitoshi Gomi, Kei Hirose, Yasuo Ohishi
Citation	Geophysical Research Letters, Volume 49, Issue 5,
Pub. date	2022, 2
Copyright	An edited version of this paper was published by AGU. Copyright 2022 American Geophysical Union.
DOI	http://dx.doi.org/10.1029/2021GL096260

Geophysical Research Letters[®]

RESEARCH LETTER

10.1029/2021GL096260

Key Points:

- We obtained the P - V - T equation of state of FeH based on volume measurements up to 142 GPa and 3660 K using a diamond-anvil cell
- ΔV_{H} , the volume increase of Fe by H atom, was determined as functions of P and T , enabling estimates of the H content in non-magnetic FeHx
- We estimate the maximum H content in the inner core and discuss the possible compositional range of the Fe-H-Si-S inner core

Supporting Information:

Supporting Information may be found in the online version of this article.

Correspondence to:

S. Tagawa,
shoh@elsi.jp

Citation:

Tagawa, S., Gomi, H., Hirose, K., & Ohishi, Y. (2022). High-temperature equation of state of FeH: Implications for hydrogen in Earth's inner core. *Geophysical Research Letters*, 49, e2021GL096260. <https://doi.org/10.1029/2021GL096260>

Received 21 SEP 2021

Accepted 22 FEB 2022

Author Contributions:

Conceptualization: Shoh Tagawa, Kei Hirose

Data curation: Shoh Tagawa

Formal analysis: Shoh Tagawa, Hitoshi Gomi

Funding acquisition: Kei Hirose

Investigation: Shoh Tagawa, Hitoshi Gomi, Yasuo Ohishi

Methodology: Shoh Tagawa, Hitoshi Gomi, Yasuo Ohishi

Project Administration: Kei Hirose, Yasuo Ohishi

Resources: Hitoshi Gomi, Kei Hirose, Yasuo Ohishi

Supervision: Kei Hirose

Validation: Shoh Tagawa, Hitoshi Gomi, Kei Hirose

Visualization: Shoh Tagawa, Hitoshi Gomi

© 2022. American Geophysical Union.
All Rights Reserved.

High-Temperature Equation of State of FeH: Implications for Hydrogen in Earth's Inner Core

Shoh Tagawa^{1,2} , Hitoshi Gomi¹ , Kei Hirose^{1,2} , and Yasuo Ohishi³

¹Earth-Life Science Institute, Tokyo Institute of Technology, Tokyo, Japan, ²Department of Earth and Planetary Science, The University of Tokyo, Tokyo, Japan, ³Japan Synchrotron Radiation Research Institute, Sayo-gun, Japan

Abstract While hydrogen is one of plausible major light elements in the core, the high-temperature equation of state (EoS) of Fe-H alloy has not been experimentally examined to the core pressure range. Here we measured the volume (V) of non-magnetic (NM) face-centered cubic (fcc) FeH at high pressure and temperature (P - T) to 142 GPa and 3660 K in a laser-heated diamond-anvil cell and obtained its P - V - T EoS. An increase in the lattice volume of Fe per H atom, ΔV_{H} , determined as functions of P and T is found to be substantially smaller than the volume of metallic H that has been used to estimate H concentration in Fe-H alloy. The ΔV_{H} is almost identical between fcc and double hexagonal close-packed phases in the NM state, suggesting that it may be applicable to hcp. The extrapolation of ΔV_{H} to inner core conditions indicates its maximum H content to be 0.8–0.9 wt%.

Plain Language Summary FeH is an important component in terrestrial planetary cores, and its equation of state (EoS) is useful to estimate their H concentrations from observed densities. The high- T EoS of FeH has not been examined experimentally to the Earth's core pressure range (>136 GPa) because of difficulties in high P - T experiments on H-bearing systems. The face-centered cubic (fcc) structure is known to be a stable form of FeH under a wide P - T range. Also, our first-principles calculations showed that fcc FeH loses the local spin moment above ~ 40 GPa. The present experiments determined the volume of fcc FeH to 142 GPa and 3660 K and obtained its EoS for the non-magnetic state. The lattice volume of Fe expands by incorporating H in its interstitial site. Our data show that ΔV_{H} , the volume increase per H atom, is similar between the fcc and double hexagonal close-packed phases in the absence of magnetism and may be applicable to hcp. Such ΔV_{H} obtained as functions of P and T predicts the density of FeHx under inner core conditions and gives the possible compositional range of the Fe-H-Si-S inner core.

1. Introduction

Hydrogen could be one of major light elements in planetary iron cores and has attracted much attention recently (see Hirose et al., 2021 for a review). Recent experimental and computational studies of metal-silicate partitioning of H showed that a large amount of H equivalent to that in 30–70 times Earth's ocean mass of water could have been distributed into the core during its formation (Li et al., 2020; Tagawa et al., 2021; Yuan & Steinle-Neumann, 2020). Indeed, the density and seismic velocity of both the outer and inner core can be reconciled with H-rich Fe alloys (Umehoto & Hirose, 2015, 2020; Wang et al., 2021). In addition, recent seismic observations of the Martian core indicate that its density is relatively low, possibly suggesting the presence of 1–2 wt% H (Stähler et al., 2021). Hydrogen in the cores of such terrestrial planets may have derived from water that was transported from an outer region of the solar system (Raymond & Morbidelli, 2020) and from proto-solar nebular gas (Ikoma & Genda, 2006; Olson & Sharp, 2019). The amount of H in the core is a key to better understanding the processes of planetary formation.

In order to constrain the H content in metallic cores, the EoS of Fe-H alloy is of great importance. While it has been reported by theory to inner core conditions (Caracas, 2015), its experimental determination has been challenging because (a) Fe has negligible solubility of H at 1 bar (e.g., Fukai & Suzuki, 1986) and (b) H concentration in Fe-H alloy therefore needs to be estimated under pressure. The EoS of stoichiometric FeH has been examined by X-ray diffraction (XRD) measurements under high pressure but only at room temperature (Badding et al., 1991; Hirao et al., 2004; Kato et al., 2020; Narygina et al., 2011; Pépin et al., 2014), except for multi-anvil experiments performed up to 21 GPa and 1573 K (Sakamaki et al., 2009). The EoSs obtained by these earlier

Writing – original draft: Shoh Tagawa, Hitoshi Gomi
Writing – review & editing: Shoh Tagawa, Hitoshi Gomi, Kei Hirose, Yasuo Ohishi

studies differ from each other because of the differences in crystal structure (dhcp and fcc) and magnetic state (ferromagnetic, FM and NM).

The volume increase of Fe per H atom, ΔV_H , provides the density of an Fe-H alloy since the lattice volume of iron expands proportionally to the amount of H (Caracas, 2015). In addition, the ΔV_H has been widely used to estimate H concentration in Fe-H alloys (Fukai, 1992; Tagawa et al., 2021; Thompson et al., 2018). Originally Fukai (1992) employed ΔV_H from the volume of metallic H (Chakravarty et al., 1981). Recent neutron diffraction measurements directly gave ΔV_H at high P - T (Machida et al., 2014, 2019; Ikuta et al., 2019), but the pressure range for such neutron diffraction studies has been limited to 12 GPa, much lower than Earth's core conditions. The temperature effect on ΔV_H remains primarily unknown (Wang et al., 2021).

In this study, we examined fcc stoichiometric FeH at high P - T based on experiment and theory. The first-principles calculations were performed in order to confirm that the magnetic state of FeH is NM under conditions of the present volume measurements at high temperatures. The thermal EoS is obtained for the NM state by measuring the volume up to 146 GPa/300 K and 119 GPa/3720 K in a laser-heated DAC. By comparing its volume with that of pure Fe, we obtain $\Delta V_H(P, T)$ as functions of P and T and discuss H concentration in the Earth's inner core. Such $\Delta V_H(P, T)$ is also useful to estimate the H content in Fe-H alloys in-situ at high P - T .

2. Experimental Methods

High P - T experiments were performed in a laser-heated DAC (Figures 1a and 1b). Three separate runs were carried out using beveled anvils with 120 and 300 μm culet sizes. A Re gasket was preindented to about 25 μm thick. Sample configuration was similar to that in Tagawa et al. (2016). In order to prevent hydrogen loss to the Re gasket, we employed a NaCl inner gasket prepared with a Focused Ion Beam. The surface of the diamond anvils was coated with a thin layer of Ti by sputtering (Ohta et al., 2015). We loaded a ~ 10 μm thick pure Fe foil ($>99.999\%$ purity, Toho Zinc) being sandwiched by thin NaCl plates that were used as a pressure marker. Only in run #3, a KCl pellet was placed between NaCl and Fe on one side as an additional pressure standard. After drying a whole DAC with the sample in it in an oven, we loaded liquid H using a liquid hydrogen-introducing system at temperatures below 20 K (Chi et al., 2011; Tagawa et al., 2016).

After compression to 15–30 GPa, dhcp FeH was synthesized by laser heating to ~ 1000 K under hydrogen-saturated conditions in a DAC. High-temperature experiments above 60 GPa under such hydrogen-saturated conditions will form FeH_2 and FeH_3 from FeH and H_2 (Pépin et al., 2014). Therefore, after synthesizing FeH at such pressure range, we fully released pressure at liquid nitrogen temperature (~ 85 K) in an N_2 atmosphere, removed excess hydrogen from a sample chamber while maintaining FeH, and repressurized the sample to >5 GPa under cryogenic temperature. It is known that metastable FeH is quenchable to 1 bar at low temperatures and begins to decompose and release hydrogen above ~ 200 K (see Figure 2 in Antonov et al., 2019). No excess hydrogen remained in the sample chamber, which is supported by the fact that neither FeH_2 nor FeH_3 was formed upon heating in their stability fields (Pépin et al., 2014). During recompression, the volume of the dhcp phase was obtained at 300 K each time with thermal annealing to ~ 1000 – 1400 K. We then heated the sample to >1500 K at ~ 40 – 60 GPa and observed a complete transformation from dhcp to fcc FeH (Isaev et al., 2007; Kato et al., 2020; Thompson et al., 2018) (Figure 2).

Structural determination and volume measurement were made on the basis of in-situ high P - T XRD spectra obtained at BL10XU, SPring-8 (Hirao et al., 2020). The incident X-ray beam was monochromatized to a wavelength of 0.41331–0.41463 \AA (~ 30 keV) and focused to 6 μm in diameter. We collected diffraction data on a flat panel X-ray detector (PerkinElmer). The sample was heated from both sides with a couple of 100 W single-mode Yb fiber lasers. A laser beam was converted to one with a flat energy distribution by beam-shaping optics, and the laser-heated spot was 30–40 μm across. Sample temperature, T_{sample} , is an average for both sides of the sample. The temperature at each side is also averaged over 6–8 μm area at a laser-heated hot spot, which corresponds to the X-ray beam size. We consider the temperature uncertainty to be $\pm 5\%$ according to Mori et al. (2017). Pressure was determined from the unit-cell volume of NaCl (pressure medium) using its thermal EoS (Dorogokupets & Dewaele, 2007). We followed Campbell et al. (2009) to estimate the effective temperature of the pressure medium; $T_{\text{NaCl}} = (3 \times T_{\text{sample}} + 300)/4 \pm (T_{\text{sample}} - 300)/4$. Such pressure at high temperature has been validated by estimates using both NaCl and KCl pressure standards in run #3. KCl may give pressures more accurately in particular when a pressure marker plays also as a pressure medium and thus its temperature variation is relatively

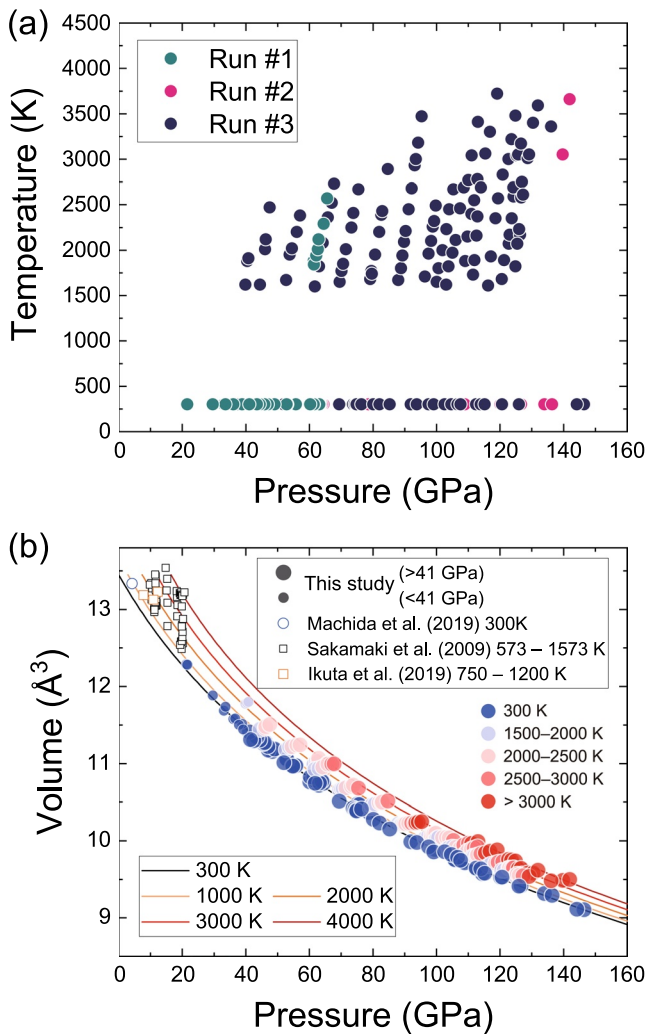


Figure 1. (a) P - T conditions for measuring the volume of FeH in runs #1–3. (b) P - V data for face-centered cubic FeH at 300 K and high temperatures. Closed large circles, this study; small open circle, Machida et al. (2019) at 300 K; black squares, Sakamaki et al. (2009) at 573–1573 K; yellow squares, Ikuta et al. (2019) at 750–1200 K. Errors in pressure and volume are presented in Dataset S1. Isothermal compression curves are for the non-magnetic state stable above ~ 40 GPa. They deviate from previous low-pressure measurements on the ferromagnetic and paramagnetic (with local spin moment) states.

large, because the thermal expansivity of KCl is much smaller than that of NaCl. We found that the pressures from NaCl are almost identical with those calculated by using the EoS of KCl proposed by Tateno et al. (2019) (Figure S1 in Supporting Information S1).

3. Results

The P - V - T data of fcc FeH were collected in a wide P - T range up to 146 GPa in P and 3720 K in T (Figure 1a and Dataset S1). Melting was not observed even at such high temperatures. It is possible that the melting temperature of stoichiometric FeH is much higher than that of FeH $_x$ ($1 < x < 2$; Hirose et al., 2019) above 40 GPa, which is supported by the recent experiments performed by Piet et al. (2021). Also, it is most unlikely that hydrogen escaped from the sample during heating because its lattice volumes obtained after heating at 300 K are always plotted on a single compression curve (Figure 1b). We employ volume data obtained only at high temperatures or at 300 K after heating, in order to avoid the effect of deviatoric stress on a sample. The fcc phase observed here was formed from dhcp FeH (Figure 2). Both phases should be stoichiometric FeH because their volumes are consistent with those of what were synthesized under hydrogen-saturated conditions (Kato et al., 2020; Pépin et al., 2014; Figure S2 in Supporting Information S1). The fcc phase being stoichiometric FeH in this study is also supported by the fact that its volume agrees with that formed in the presence of excess H $_2$ in Kato et al. (2020). The volume of dhcp FeH was measured in run #1 at 22–61 GPa (Dataset S1).

Our total energy calculations demonstrate that the FM state is stable for fcc FeH at ambient pressure and the FM-NM transition occurs at 47 GPa and 0 K (see text in the, Figure S3b in Supporting Information S1). The FM state changes to PM above the Curie temperature, which rapidly decreases with compression (Figure S3c in Supporting Information S1). The local spin moment of the PM state will be quenched at the volume larger than that for FM (Figure S3a in Supporting Information S1), indicating that the PM fcc FeH is also expected to lose its local spin moment at pressure lower than 47 GPa.

The present P - V data of fcc FeH obtained at 300 K are compared with the compression curves previously reported by experiments for the dhcp and fcc phases (Badding et al., 1991; Hirao et al., 2004; Kato et al., 2020; Narygina et al., 2011; Pépin et al., 2014; Figure S2 in Supporting Information S1). Deviations among these studies including the present one may be attributed to the difference in the magnetic state, resulting from different crystal structure, as well as thermal annealing during compression. The extrapolated compression curves reported by Hirao et al. (2004) and Narygina et al. (2011) disagree with ours because volumes were measured in limited pressure ranges in these two earlier experiments.

Here we obtain the room-temperature Vinet P - V EoS for the NM state by using the present 300 K data collected only above 41 GPa considering the pressure uncertainty in our first-principles calculations;

Here we obtain the room-temperature Vinet P - V EoS for the NM state by using the present 300 K data collected only above 41 GPa considering the pressure uncertainty in our first-principles calculations;

$$P = 3K_{0,300\text{K}} \left(\frac{V}{V_{0,300\text{K}}} \right)^{-2/3} \left[1 - \left(\frac{V}{V_{0,300\text{K}}} \right)^{1/3} \right] \exp \left\{ \frac{3}{2} (K'_{0,300\text{K}} - 1) \left[1 - \left(\frac{V}{V_{0,300\text{K}}} \right)^{1/3} \right] \right\} \quad (1)$$

High-temperature (>1600 K) FeH data were acquired for the NM state above 41 GPa in this study (Figure 1a). These data are fitted by the Mie-Grüneisen-Debye model (e.g., Dewaele et al., 2006);

$$P_{th}(V, T) = \frac{\gamma(V)}{V} \{ E_{th}(T, V) - E_{th}(300\text{K}, V) \} \quad (2)$$

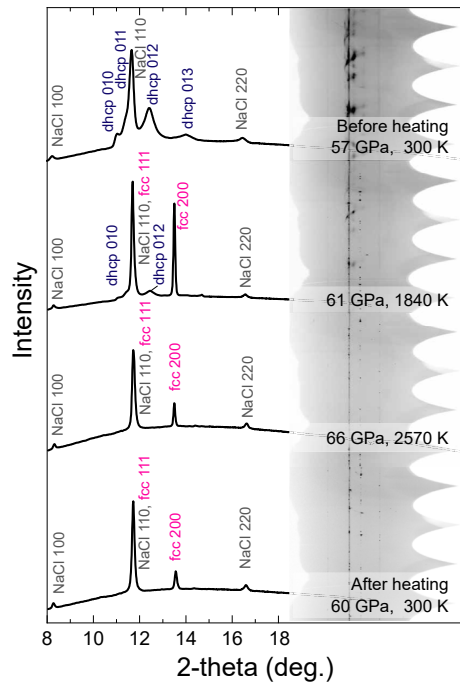


Figure 2. X-ray diffraction data collected in run #1 before heating for double hexagonal close-packed FeH and during/after heating for the face-centered cubic phase.

$$E_{th} = 9nk_B \left(\frac{\Theta_D}{8} + T \left(\frac{T}{\Theta_D} \right)^3 \int_0^{\Theta_D/T} \frac{x^3}{\exp(x) - 1} dx \right) \quad (3)$$

$$\Theta_D = \Theta_0 x^{-\gamma_\infty} \exp \left[\frac{\gamma_0 - \gamma_\infty}{\beta} (1 - x^\beta) \right] \quad (4)$$

$$\beta = \frac{\gamma_0}{\gamma_0 - \gamma_\infty} \quad (5a)$$

$$\gamma(V) = \gamma_\infty + (\gamma_0 - \gamma_\infty)x^\beta \quad (5b)$$

where E_{th} is thermal energy, γ is Grüneisen parameter (subscript 0 and ∞ denote values at ambient and infinitely compressed conditions, respectively), Θ_D is Debye temperature, n is the number of atoms per formula unit ($n = 2$ for FeH), k_B is Boltzmann's constant in $\text{GPa} \cdot \text{\AA}^3 \cdot \text{K}^{-1}$ unit, and β is a fitted parameter. Θ_D is also formulated from the Debye sound velocity as;

$$\Theta_D = \frac{h}{2\pi k_B} \left(\frac{6\pi^2 N}{V} \right)^{\frac{1}{3}} v_D \quad (6)$$

where h is Planck's constant and v_D is Debye sound speed. We estimated Θ_0 , γ_0 , and γ_∞ to be consistent with both our P - V - T data and v_D reported by Thompson et al. (2018) from NRIXS measurements above 41 GPa. These fittings provide $V_0 = 13.45(15) \text{\AA}^3$ for a formula unit, $K_0 = 183(20) \text{ GPa}$, $K' = 3.84(37)$, $\Theta_0 = 758 \text{ K}$ (fixed), $n = 2$, $\gamma_0 = 0.738(40)$, and $\gamma_\infty = 0.547(83)$. These parameters are compared with those for fcc pure Fe (Tsujino et al., 2013) and for dhcp FeH based on data collected below 20 GPa (Sakamaki et al., 2009) in Table S1 in Supporting Information S1. The present EoS for the NM state predicts smaller volumes than observed by Sakamaki et al. (2009) for the FM and possibly PM (with local spin moment) states at

<21 GPa and high temperatures to 1573 K (Figure 1b).

4. Discussion

4.1. ΔV_H at High P and T

We obtain ΔV_H from the difference in volume between FeH and Fe. Here we employ the EoSs of fcc and hcp Fe for the NM state reported by Dorogokupets et al. (2017), in which pressure was calibrated to be consistent with the NaCl scale by Dorogokupets and Dewaele (2007) that is employed in this study. The room-temperature ΔV_H for both fcc and dhcp FeH is shown as a function of pressure in Figure 3a. The volume of dhcp FeH was obtained in run #1 between 22 and 57 GPa, and ΔV_{H_dhcp} is calculated by using the volume of hcp Fe which is similar in structure to dhcp. ΔV_{H_dhcp} is larger than ΔV_{H_fcc} for the fcc phase at relatively low pressures, which is also evident from neutron diffraction experiments at <5 GPa (Machida et al., 2014; Ikuta et al., 2019; Antonov et al., 1998). Nevertheless, ΔV_{H_dhcp} decreases more rapidly than ΔV_{H_fcc} with compression, and both become similar above 45 GPa. Such behavior of ΔV_{H_dhcp} is likely attributed to the FM to NM transition in dhcp FeH (Ying et al., 2020). Also, ΔV_{H_fcc} data below 40 GPa including neutron diffraction data at 4.2 GPa are for the FM and possibly PM (with local spin moment) states and larger than that for its NM state (Figure 3a). It is noted that once Fe loses its local spin moment, ΔV_{H_fcc} and ΔV_{H_dhcp} are found to be almost identical with each other, suggesting that ΔV_H determined for the fcc NM state may be applicable to hcp Fe-H alloys.

The present experiments give not only the pressure effect but also the temperature dependence of $\Delta V_H(P, T)$ for the NM state (Figure 3b), which has not been demonstrated previously except for the recent calculations by Wang et al. (2021) performed only at 360 GPa and 2000–6500 K (Figure 3c). It is different from that with the local spin moment, which was previously reported at pressures less than 12 GPa (Ikuta et al., 2019). As demonstrated in these figures, ΔV_H diminishes with increasing temperature likely because the interstitial sites for H around

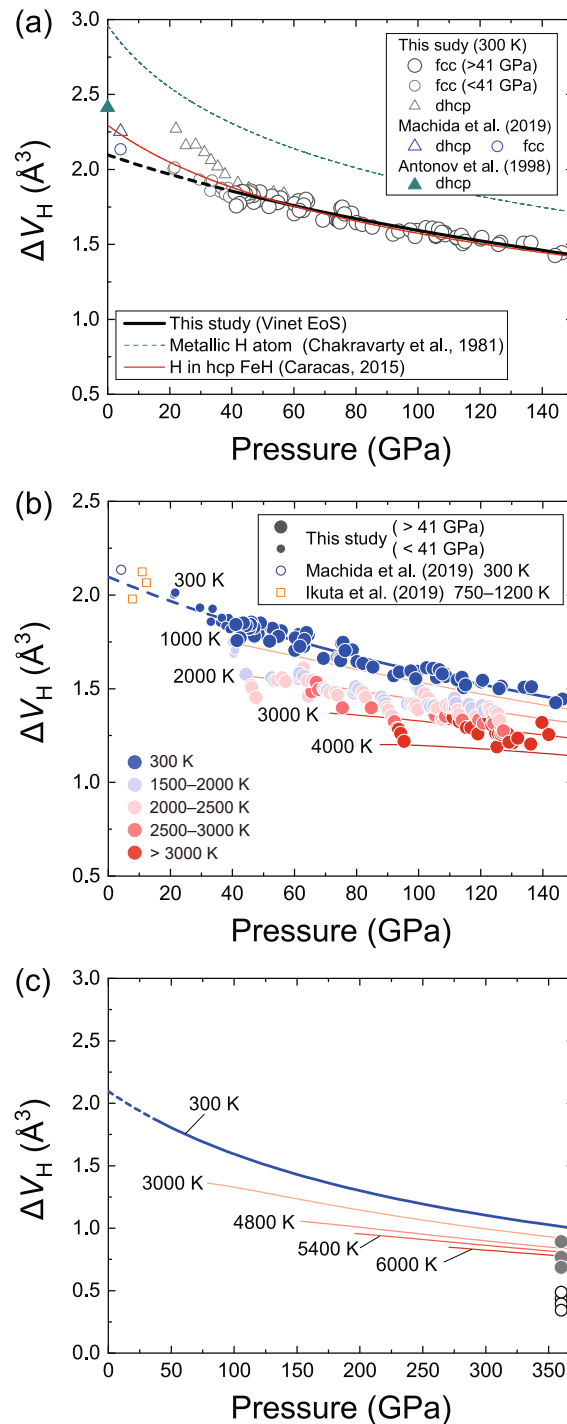


Figure 3. ΔV_H obtained in the present experiments. (a) ΔV_H at 300 K and high pressures found for face-centered cubic (fcc) (circles) and double hexagonal close-packed (triangles) FeH (black solid line). Data by neutron diffraction measurements at low pressures are from Machida et al. (2019) (blue) and Antonov et al. (1998) (green). Large and small symbols represent the data for non-magnetic (NM) and ferromagnetic (FM) (or paramagnetic (PM) with local spin moment) states, respectively. They are much smaller than the calculated volume of metallic H (Chakravarty et al., 1981) (or paramagnetic (PM) with local spin moment) states, which was employed by Fukai (1992) to estimate H concentration in Fe-H alloys. The present data for NM fcc FeH is consistent with the ΔV_H theoretically calculated for hcp FeH at 0 K by Caracas (2015) (red line). (b) Changes in ΔV_H for NM (large circles) and FM (or PM with local spin moment) (small circles and squares) fcc FeH at high pressures with increasing temperature. Neutron diffraction data (open symbols) are given for 300 K (Machida et al., 2019) and 750–1200 K (Ikuta et al., 2019). Colored curves indicate the effect of temperature from 300 to 4000 (K) (c) ΔV_H extrapolated to inner core P - T (colored curves). Data for hcp $\text{Fe}_{60}\text{Si}_4\text{H}_8$ (gray circles) and Fe_{64}H_4 (open circles) by first-principles calculations (Wang et al., 2021) are also plotted.

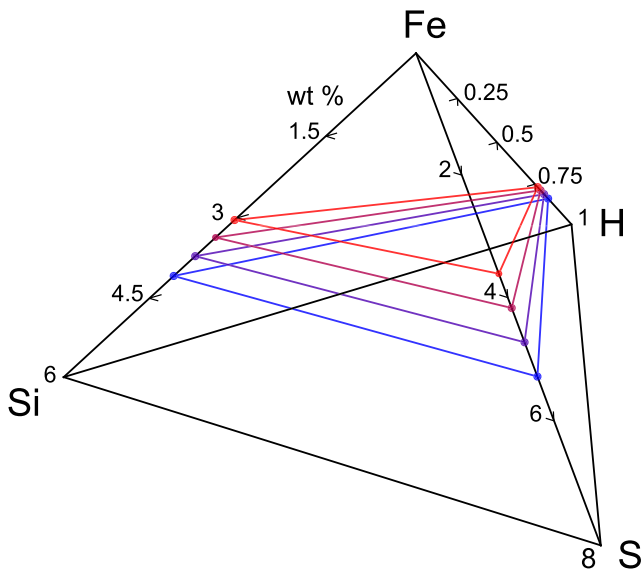


Figure 4. Possible ranges of the Fe-H-Si-S inner composition illustrated by each triangle plane depending on inner core boundary temperature (blue, 4800 K; purple, 5400 K; magenta, 6000 K; red, 6600 K).

Fe atoms expand at high temperature; the ΔV_H decreases by about 10% at 2000 K in a wide pressure range and by 16%–20% at inner core boundary (ICB) conditions of 330 GPa and 5400–6000 K.

Fitting Vinet EoS (Equation 1) to $\Delta V_{H_{fcc}}$ data at 300 K for NM FeH gives $V_0 = 2.097(1) \text{ \AA}^3$, $K_0 = 301.2(9) \text{ GPa}$, and $K' = 1.404(6)$. And, the temperature effect can be approximated as; $\Delta V_{H_{fcc}}(P, T) = -0.00241(1) \times P - 1.338(13) \times 10^{-4} \times T + 2.724(46) \times 10^{-7} \times P \times T + 1.872(3)$ (Figure 3b). This equation predicts ΔV_H that deviates by less than 0.1 \AA from our experimental data at >60 GPa and 300–6600 K.

At 0–300 K, both $\Delta V_{H_{dhcp}}$ and $\Delta V_{H_{fcc}}$ observed here are remarkably smaller than the volume of metallic hydrogen, $\Delta V_{\text{metal-H}}$ (Figure 3a), which was calculated considering a close-packed structure and vibrational contributions by Chakravarty et al. (1981). The $\Delta V_{\text{metal-H}}$ was originally employed by Fukai (1992) and has been used to calculate H concentration in Fe-H alloys (e.g., Shibasaki et al., 2011; Terasaki et al., 2012). However, they were always underestimated by several tens % since $\Delta V_{\text{metal-H}}$ is substantially larger than ΔV_H in FeH. In contrast, the $\Delta V_{H_{fcc}}$ at room temperature is approximately consistent with that previously calculated at 0 K by Caracas (2015). When our $\Delta V_{H_{fcc}}$ is extrapolated to high P - T conditions for the Earth's inner core (330–364 GPa, >4800 K), it is broadly consistent with $\Delta V_{H_{hcp}}$ obtained for hcp $\text{Fe}_{60}\text{Si}_4\text{H}_8$ by first-principles calculations (Wang et al., 2021), although their calculations for Fe_{64}H_4 gave smaller values (Figure 3c).

4.2. Implications for Hydrogen in Earth's Inner Core

Hydrogen can be an important light impurity element in the Earth's outer core to explain its density and seismic velocity (Umehoto & Hirose, 2015, 2020). Previous multi-anvil experiments performed at 15–20 GPa demonstrated the solid-Fe/liquid-Fe partition coefficient of H, D_H (solid/liquid) to be ~ 0.7 by weight (Imai, 2013), indicating that hydrogen could be a major light element in the solid inner core as well. Indeed, the recent calculations by Wang et al. (2021) demonstrated that the inner core may include up to 0.23 wt% H together with Si, depending on its temperature, to explain the observed density and velocities simultaneously.

Independently from earlier estimates, we can constrain H concentration in the inner core based on $\Delta V_H(P, T)$ obtained above. If hydrogen is a sole light element, the inner core density is explained with 0.8–0.9 wt% H (0.78–0.85 wt% H at the ICB) considering its temperatures to be 4800–6600 K (Figure 4). We note that such estimate of the H content is almost independent on temperature, because the higher the inner core temperature is, the smaller the density deficit with respect to pure Fe is, but ΔV_H also becomes smaller (Figure 3c). It is not the case for silicon nor sulfur, another plausible light elements in the inner core. With the thermal EoSs of hcp Fe-9wt%Si alloy (Fischer et al., 2014) and Fe (Dorogokupets et al., 2017), the amount of Si required to explain the inner core density deficit as a single light element is estimated to be 4.1 wt% at the ICB pressure of 330 GPa and 4800 K, which decreases to 3.1 wt% with increasing temperature to 6600 K (Figure 4). Also, the experiments performed by Sakai et al. (2012) on an Fe-Ni-S alloy demonstrated that 5.3 to 3.6 wt% S explains the density at the inner core side of the ICB when the effect of nickel is not considered, depending on its temperature ranging from 4800 to 6600 K.

The Earth's inner core should be an Fe-H-Si-S (-Ni) alloy with least amounts of C and O because their solid-Fe/liquid-Fe partition coefficients are limited to 0–0.1 (Alfè et al., 2002; Hasegawa et al., 2021; Li et al., 2019; Ozawa et al., 2010). If the excess volume of mixing is negligible, the inner core composition may be represented by a mixture among Fe-0.85 wt% H, Fe-4.1 wt% Si, and Fe-5.3 wt% S when the ICB temperature is 4800 K. The possible ranges of the Fe-H-Si-S inner core composition are illustrated in Figure 4, depending on the ICB temperature ranging from 4800 to 6600 K. Furthermore, such possible ranges of the inner core composition can constrain the possible liquid outer core composition, once the partitioning of light elements between the outer and inner core is better understood including their interactions (e.g., Hirose et al., 2021; Tao & Fei, 2021; Tateno et al., 2018).

5. Conclusions

We constructed the high-temperature EoS of fcc FeH in the NM state based on its volume measurements of fcc FeH were carried out to 142 GPa and 3660 K in a laser-heated DAC, in which we avoided the formation of FeH₂ and FeH₃ by releasing excess H₂ from a sample chamber after the synthesis of stoichiometric FeH. According to our first-principles calculations, we employed data only above 41 GPa that represent the NM state. The EoS of FeH provides $\Delta V_H(P, T)$, the volume increase per H atom, for Fe-H alloys as functions of P and T , which we found is similar between fcc and dhcp at NM conditions and may therefore be applicable to hcp as well. Such $\Delta V_H(P, T)$ is remarkably smaller than the volume of metallic H at equivalent conditions and will be useful for in-situ quantification of H contents in Fe-H alloys under P - T . When extrapolated to inner core conditions, our $\Delta V_H(P, T)$ is in broad agreement with that by recent theoretical predictions (Wang et al., 2021). It gives the maximum H content in the inner core to be 0.8–0.9 wt%, which is almost independent of temperature because the higher the inner core temperature is, the smaller the density deficit is, but $\Delta V_H(P, T)$ also decreases. We also estimated the possible compositional range of the Fe-H-Si-S inner core.

Data Availability Statement

Datasets for this research are found in Dataset S1 available online (from <https://doi.org/10.5281/zenodo.5513718>).

Acknowledgments

Discussion with G. Helffrich on the magnetic state of FeH was valuable. We thank S. Tateno and K. Ohta for their support in our experiment. Comments from two anonymous referees helped to improve the paper. Synchrotron XRD measurements were made at BL10XU, SPring-8 (proposals No. 2018B0072, 2019A0072, and 2019B0072). This work was supported by the Japan Society for the Promotion of Science grants.

References

- Alfè, D., Gillan, M. J., & Price, G. D. (2002). Composition and temperature of the Earth's core constrained by combining ab initio calculations and seismic data. *Earth and Planetary Science Letters*, 195(1–2), 91–98. [https://doi.org/10.1016/S0012-821X\(01\)00568-4](https://doi.org/10.1016/S0012-821X(01)00568-4)
- Antonov, V. E., Cornell, K., Fedotov, V. K., Kolesnikov, A. I., Ponyatovsky, E. G., Shiryaev, V. I., & Wipf, H. (1998). Neutron diffraction investigation of the dhcp and hcp iron hydrides and deuterides. *Journal of Alloys and Compounds*, 264(1–2), 214–222. [https://doi.org/10.1016/S0925-8388\(97\)00298-3](https://doi.org/10.1016/S0925-8388(97)00298-3)
- Antonov, V. E., Gurev, V. M., Kulakov, V. I., Kuzovnikov, M. A., Sholin, I. A., & Zuykova, V. Y. (2019). Solubility of deuterium and hydrogen in fcc iron at high pressures and temperatures. *Physical Review Materials*, 3(11), 113604. <https://doi.org/10.1103/PhysRevMaterials.3.113604>
- Badding, J. V., Hemley, R. J., & Mao, H. K. (1991). High-pressure chemistry of hydrogen in metals: In situ study of iron hydride. *Science*, 253(5018), 421–424. <https://doi.org/10.1126/science.253.5018.421>
- Campbell, A. J., Danielson, L., Righter, K., Seagle, C. T., Wang, Y., & Prakapenka, V. B. (2009). High pressure effects on the iron-iron oxide and nickel-nickel oxide oxygen fugacity buffers. *Earth and Planetary Science Letters*, 286(3–4), 556–564. <https://doi.org/10.1016/j.epsl.2009.07.022>
- Caracas, R. (2015). The influence of hydrogen on the seismic properties of solid iron. *Geophysical Research Letters*, 42(10), 3780–3785. <https://doi.org/10.1002/2015GL063478>
- Chakravarty, S., Rose, J. H., Wood, D., & Ashcroft, N. W. (1981). Theory of dense hydrogen. *Physical Review B*, 24(4), 1624–1635. <https://doi.org/10.1103/PhysRevB.24.1624>
- Chi, Z., Nguyen, H., Matsuoka, T., Kagayama, T., Hirao, N., Ohishi, Y., & Shimizu, K. (2011). Cryogenic implementation of charging diamond anvil cells with H₂ and D₂. *Review of Scientific Instruments*, 82(10), 105109. <https://doi.org/10.1063/1.3652981>
- Dewaele, A., Loubeyre, P., Ocellli, F., Mezouar, M., Dorogokupets, P. I., & Torrent, M. (2006). Quasihydrostatic equation of state of iron above 2 Mbar. *Physical Review Letters*, 97(21), 215504. <https://doi.org/10.1103/PhysRevLett.97.215504>
- Dorogokupets, P. I., & Dewaele, A. (2007). Equations of state of MgO, Au, Pt, NaCl-B1, and NaCl-B2: Internally consistent high-temperature pressure scales. *High Pressure Research*, 27(4), 431–446. <https://doi.org/10.1080/08957950701659700>
- Dorogokupets, P. I., Dymshits, A. M., Litasov, K. D., & Sokolova, T. S. (2017). Thermodynamics and equations of state of iron to 350 GPa and 6000 K. *Scientific Reports*, 7(1), 41863. <https://doi.org/10.1038/srep41863>
- Fischer, R. A., Campbell, A. J., Caracas, R., Reaman, D. M., Heinz, D. L., Dera, P., & Prakapenka, V. B. (2014). Equations of state in the Fe-FeSi system at high pressures and temperatures. *Journal of Geophysical Research: Solid Earth*, 119(4), 2810–2827. <https://doi.org/10.1002/2013JB010898>
- Fukai, Y. (1992). Some properties of the Fe-H system at high pressures and temperatures, and their implications for the Earth's core. In Y. Syono & M. H. Manghnani (Eds.), *High-Pressure Research: Application to Earth and Planetary Sciences, Geophysical Monograph Series* (Vol. 67, pp. 373–385). <https://doi.org/10.1029/GM067p0373>
- Fukai, Y., & Suzuki, T. (1986). Iron–water reaction under high pressure and its implication in the evolution of the Earth. *Journal of Geophysical Research*, 91(B9), 9222–9230. <https://doi.org/10.1029/JB091iB09p09222>
- Hasegawa, M., Hirose, K., Oka, K., & Ohishi, Y. (2021). Liquidus phase relations and solid-liquid partitioning in the Fe-Si-C system under core pressures. *Geophysical Research Letters*, 48(13), e2021GL092681. <https://doi.org/10.1029/2021gl092681>
- Hirao, N., Kawaguchi, S. I., Hirose, K., Shimizu, K., Ohtani, E., & Ohishi, Y. (2020). New developments in high-pressure X-ray diffraction beam-line for diamond anvil cell at SPring-8. *Matter and Radiation at Extremes*, 5(1), 1–10. <https://doi.org/10.1063/1.5126038>
- Hirao, N., Kondo, T., Ohtani, E., Takemura, K., & Kikegawa, T. (2004). Compression of iron hydride to 80 GPa and hydrogen in the Earth's inner core. *Geophysical Research Letters*, 31(6), L06616. <https://doi.org/10.1029/2003GL019380>
- Hirose, K., Tagawa, S., Kuwayama, Y., Sinmyo, R., Morard, G., Ohishi, Y., & Genda, H. (2019). Hydrogen limits carbon in liquid iron. *Geophysical Research Letters*, 46(10), 5190–5197. <https://doi.org/10.1029/2019GL082591>
- Hirose, K., Wood, B., & Vočadlo, L. (2021). Light elements in the Earth's core. *Nature Reviews Earth & Environment*, 2(9), 645–658. <https://doi.org/10.1038/s43017-021-00203-6>
- Ikoma, M., & Genda, H. (2006). Constraints on the mass of a habitable planet with water of nebular origin. *The Astrophysical Journal*, 648(1), 696–706. <https://doi.org/10.1086/505780>

- Ikuta, D., Ohtani, E., Sano-Furukawa, A., Shibazaki, Y., Terasaki, H., Yuan, L., & Hattori, T. (2019). Interstitial hydrogen atoms in face-centered cubic iron in the Earth's core. *Scientific Reports*, 9(1), 7108. <https://doi.org/10.1038/s41598-019-43601-z>
- Imai, T. (2013). *Hydrogen partitioning between iron and silicate and melting phase relation in the system Fe-FeH*, (Doctoral dissertation). Tokyo Institute of Technology.
- Isaev, E. I., Skorodumova, N. V., Ahuja, R., Vekilov, Y. K., & Johansson, B. (2007). Dynamical stability of Fe-H in the Earth's mantle and core regions. *Proceedings of the National Academy of Sciences*, 104(22), 9168–9171. <https://doi.org/10.1073/pnas.0609701104>
- Kato, C., Umemoto, K., Ohta, K., Tagawa, S., Hirose, K., & Ohishi, Y. (2020). Stability of fcc phase FeH to 137 GPa. *American Mineralogist*, 105(6), 917–921. <https://doi.org/10.2138/am-2020-7153>
- Li, Y., Vočadlo, L., Alfè, D., & Brodholt, J. (2019). Carbon partitioning between the Earth's inner and outer core. *Journal of Geophysical Research: Solid Earth*, 124(12), 12812–12824. <https://doi.org/10.1029/2019JB018789>
- Li, Y., Vočadlo, L., Sun, T., & Brodholt, J. P. (2020). The Earth's core as a reservoir of water. *Nature Geoscience*, 13(6), 453–458. <https://doi.org/10.1038/s41561-020-0578-1>
- Machida, A., Saitoh, H., Hattori, T., Sano-Furukawa, A., Funakoshi, K., Sato, T., et al. (2019). Hexagonal close-packed iron hydride behind the conventional phase diagram. *Scientific Reports*, 9(1), 12290. <https://doi.org/10.1038/s41598-019-48817-7>
- Machida, A., Saitoh, H., Sugimoto, H., Hattori, T., Sano-Furukawa, A., Endo, N., et al. (2014). Site occupancy of interstitial deuterium atoms in face-centred cubic iron. *Nature Communications*, 5(1), 5063. <https://doi.org/10.1038/ncomms6063>
- Mori, Y., Ozawa, H., Hirose, K., Sinmyo, R., Tateno, S., Morard, G., & Ohishi, Y. (2017). Melting experiments on Fe-Fe₃S system to 254 GPa. *Earth and Planetary Science Letters*, 464, 135–141. <https://doi.org/10.1016/j.epsl.2017.02.021>
- Narygina, O., Dubrovinsky, L. S., McCammon, C. A., Kurnosov, A., Kantor, I. Y., Prakapenka, V. B., & Dubrovinskaya, N. A. (2011). X-ray diffraction and Mössbauer spectroscopy study of fcc iron hydride FeH at high pressures and implications for the composition of the Earth's core. *Earth and Planetary Science Letters*, 307(3–4), 409–414. <https://doi.org/10.1016/j.epsl.2011.05.015>
- Ohta, K., Ichimaru, K., Einaga, M., Kawaguchi, S., Shimizu, K., Matsuoka, T., et al. (2015). Phase boundary of hot dense fluid hydrogen. *Scientific Reports*, 5(1), 16560. <https://doi.org/10.1038/srep16560>
- Olson, P. L., & Sharp, Z. D. (2019). Nebular atmosphere to Magma Ocean: A model for volatile capture during earth accretion. *Physics of the Earth and Planetary Interiors*, 294, 106294. <https://doi.org/10.1016/j.pepi.2019.106294>
- Ozawa, H., Hirose, K., Tateno, S., Sata, N., & Ohishi, Y. (2010). Phase transition boundary between B1 and B8 structures of FeO up to 210 GPa. *Physics of the Earth and Planetary Interiors*, 179(3–4), 157–163. <https://doi.org/10.1016/j.pepi.2009.11.005>
- Pépin, C. M., Dewaele, A., Geneste, G., Loubeyre, P., & Mezouar, M. (2014). New iron hydrides under high pressure. *Physical Review Letters*, 113(26), 265504. <https://doi.org/10.1103/PhysRevLett.113.265504>
- Piet, H., Chizmeshya, A. V. G., Chen, B., Chariton, S., Greenberg, E., Prakapenka, V. B., & Shim, S.-H. (2021). Effect of nickel on the high-pressure phases in FeH. *Physical Review B*, 104(22), 224106. <https://doi.org/10.1103/PhysRevB.104.224106>
- Raymond, S. N., & Morbidelli, A. (2020). Planet formation: Key mechanisms and global models. In *Demographics of Exoplanetary systems*, Springer. Retrieved from https://link.springer.com/chapter/10.1007/978-3-030-88124-5_1
- Sakai, T., Ohtani, E., Kamada, S., Terasaki, H., & Hirao, N. (2012). Compression of Fe_{88.1}Ni_{9.1}S_{2.8} alloy up to the pressure of Earth's inner core. *Journal of Geophysical Research*, 117(B2), B02210. <https://doi.org/10.1029/2011JB008745>
- Sakamaki, K., Takahashi, E., Nakajima, Y., Nishihara, Y., Funakoshi, K., Suzuki, T., & Fukai, Y. (2009). Melting phase relation of FeHx up to 20 GPa: Implication for the temperature of the Earth's core. *Physics of the Earth and Planetary Interiors*, 174(1–4), 192–201. <https://doi.org/10.1016/j.pepi.2008.05.017>
- Shibazaki, Y., Ohtani, E., Terasaki, H., Tateyama, R., Sakamaki, T., Tsuchiya, T., & Funakoshi, K. (2011). Effect of hydrogen on the melting temperature of FeS at high pressure: Implications for the core of Ganymede. *Earth and Planetary Science Letters*, 301(1–2), 153–158. <https://doi.org/10.1016/j.epsl.2010.10.033>
- Stähler, S. C., Khan, A., Banerdt, W. B., Lognonné, P., Giardini, D., Ceylan, S., et al. (2021). Seismic detection of the Martian core. *Science*, 373(6553), 443–448. <https://doi.org/10.1126/science.aba7730>
- Tagawa, S., Ohta, K., Hirose, K., Kato, C., & Ohishi, Y. (2016). Compression of Fe-Si-H alloys to core pressures. *Geophysical Research Letters*, 43(8), 3686–3692. <https://doi.org/10.1002/2016GL068848>
- Tagawa, S., Sakamoto, N., Hirose, K., Yokoo, S., Hernlund, J., Ohishi, Y., & Yurimoto, H. (2021). Experimental evidence for hydrogen incorporation into Earth's core. *Nature Communications*, 12(1), 2588. <https://doi.org/10.1038/s41467-021-22035-0>
- Tao, R., Fei, Y., Tateno, S., Hirose, K., Sinmyo, R., Morard, G., et al. (2021). High-pressure experimental constraints of partitioning behavior of Si and S at the Mercury's inner core boundary melting experiments on Fe-Si-S alloys to core pressures: Silicon in the core? *Earth and Planetary Science Letters* *American Mineralogist*, 562(103(5)), 116849. <https://doi.org/10.1016/j.epsl.2021.116849>
- Tateno, S., Hirose, K., Sinmyo, R., Morard, G., Hirao, N., & Ohishi, Y. (2018). Melting experiments on Fe-Si-S alloys to core pressures: Silicon in the core? *American Mineralogist*, 103(5), 742–748. <https://doi.org/10.2138/am-2018-6299>
- Tateno, S., Komabayashi, T., Hirose, K., Hirao, N., & Ohishi, Y. (2019). Static compression of B2 KCl to 230 GPa and its P-V-T equation of state. *American Mineralogist*, 104(5), 718–723. <https://doi.org/10.2138/am-2019-6779>
- Terasaki, H., Ohtani, E., Sakai, T., Kamada, S., Asanuma, H., Shibazaki, Y., et al. (2012). Stability of Fe-Ni hydride after the reaction between Fe-Ni alloy and hydrous phase (δ-AIOOH) up to 1.2 Mbar: Possibility of H contribution to the core density deficit. *Physics of the Earth and Planetary Interiors*, 194–195, 18–24. <https://doi.org/10.1016/j.pepi.2012.01.002>
- Thompson, E. C., Davis, A. H., Bi, W., Zhao, J., Alp, E. E., Zhang, D., et al. (2018). High-pressure geophysical properties of fcc phase FeHx. *Geochemistry, Geophysics, Geosystems*, 19(1), 305–314. <https://doi.org/10.1002/2017GC007168>
- Tsujino, N., Nishihara, Y., Nakajima, Y., Takahashi, E., Funakoshi, K., & Higo, Y. (2013). Equation of state of γ-Fe: Reference density for planetary cores. *Earth and Planetary Science Letters*, 375, 244–253. <https://doi.org/10.1016/j.epsl.2013.05.040>
- Umemoto, K., & Hirose, K. (2015). Liquid iron-hydrogen alloys at outer core conditions by first-principles calculations. *Geophysical Research Letters*, 42(18), 7513–7520. <https://doi.org/10.1002/2015GL065899>
- Umemoto, K., & Hirose, K. (2020). Chemical compositions of the outer core examined by first principles calculations. *Earth and Planetary Science Letters*, 531, 116009. <https://doi.org/10.1016/j.epsl.2019.116009>
- Wang, W., Li, Y., Brodholt, J. P., Vočadlo, L., Walter, M. J., & Wu, Z. (2021). Strong shear softening induced by superionic hydrogen in Earth's inner core. *Earth and Planetary Science Letters*, 568, 117014. <https://doi.org/10.1016/j.epsl.2021.117014>
- Ying, J., Zhao, J., Bi, W., Alp, E. E., Xiao, Y., Chow, P., et al. (2020). Magnetic phase diagram of ε'-FeH. *Physical Review B*, 101(2), 020405. <https://doi.org/10.1103/PhysRevB.101.020405>
- Yuan, L., & Steinle-Neumann, G. (2020). Strong sequestration of hydrogen into the Earth's core during planetary differentiation. *Geophysical Research Letters*, 47(15), e2020GL088303. <https://doi.org/10.1029/2020GL088303>

References From the Supporting Information

- Akai, H. (1989). Fast Korringa-Kohn-Rostoker coherent potential approximation and its application to fcc Ni-Fe systems. *Journal of Physics: Condensed Matter*, *1*(43), 8045–8064. <https://doi.org/10.1088/0953-8984/1/43/006>
- Akai, H., & Dederichs, P. H. (1993). Local moment disorder in ferromagnetic alloys. *Physical Review B*, *47*(14), 8739–8747. <https://doi.org/10.1103/PhysRevB.47.8739>
- Gomi, H., Fei, Y., & Yoshino, T. (2018). The effects of ferromagnetism and interstitial hydrogen on the equation of states of hcp and dhcp FeHx: Implications for the earth's inner core age. *American Mineralogist*, *103*(8), 1271–1281. <https://doi.org/10.2138/am-2018-6295>
- Perdew, J. P., Burke, K., & Ernzerhof, M. (1996). Generalized gradient approximation made simple. *Physical Review Letters*, *77*(18), 3865–3868. <https://doi.org/10.1103/PhysRevLett.77.3865>
- Sato, K., Dederichs, P. H., & Katayama-Yoshida, H. (2003). Curie temperatures of III–V diluted magnetic semiconductors calculated from first principles. *Europhysics Letters*, *61*(3), 403–408. <https://doi.org/10.1209/epl/i2003-00191-8>